Heterogeneous & Homogeneous & Bio- & Nano-
CHEMCATCHEM
CATALYSIS

Accepted Article

Title: Auto-reduction Behaviour of Cobalt on Graphitic Carbon Nitride Coated Alumina Supports for Fischer-Tropsch Synthesis

Authors: Hunmin Park, Kwang Young Kim, Duck Hyun Youn, Yo Han Choi, Won Young Kim, and Jae Sung Lee

To be cited as: *ChemCatChem* 10.1002/cctc.201700613

Link to VoR: http://dx.doi.org/10.1002/cctc.201700613

A Journal of
ChemPubSoc Europe

WILEY-VCH

www.chemcatchem.org

Auto-Reduction Behaviour of Cobalt on Graphitic Carbon Nitride Coated Alumina Supports for Fischer-Tropsch Synthesis

Hunmin Park,[†][b] Kwang Young Kim,[†][a] Duck Hyun Youn,[a] Yo Han Choi,[c] Won Young Kim,[b] and Jae Sung Lee*[a]

Abstract: The graphitic carbon nitride (g-C_3N_4)-coated alumina (CN-Al) is investigated as a support material for a cobalt-based Fischer-Tropsch synthesis (FTS) catalyst. The g-C_3N_4 blocks the interaction between cobalt and alumina to hinder the formation of irreducible cobalt oxide species, and improves the dispersion of metallic cobalt species on the CN-Al support. Furthermore, the coated g-C_3N_4 is decomposed during the pre-annealing process even under the inert condition to evolve reductive carbon monoxide gas that directly reduces the cobalt oxide species to metallic cobalt. Hence, the catalyst can be activated without typical hydrogen pretreatment. Moreover, the reduction promotion by expensive noble metals like Pt is not needed either. Because of the improved dispersion and reducibility of the cobalt species on CN-Al support, the catalytic FTS activity of Co/CN-Al is higher compared to the conventional Co/Al_2O_3 catalyst.

Introduction

Alternative fuel production from non-petroleum resources is an urgent issue today, because the petroleum has problems of long-term supply and emission of environmentally harmful exhausts to the air.[1] Technologies have been developed to substitute petroleum with electricity derived especially from renewable energies as the transportation energy like Li-ion batteries and fuel cells.[2] Another approach is XTL (X-to-liquid) process to produce liquid fuels from non-petroleum sources such as natural gas (GTL, gas-to-liquid), and coal (CTL, coal-to-liquid), which have more reserves than petroleum.[3] The liquid fuels from XTL process have advantages that current petroleum refinery facility could be used to produce derivatives of petrochemical products. Moreover, diesel or gasoline produced from syncrude could be environmentally less harmful and of better quality compared to traditional oil from petroleum.[4] The resources of XTL process could also be replaced by biomass (BTL), and organic wastes (WTL), which enable the sustainable production of liquid hydrocarbons without adding anthropogenic CO_2.[3a]

Fischer-Tropsch synthesis (FTS) is the key and common reaction in the XTL processes, which produces hydrocarbon chains from H_2 and CO mixtures (synthesis gas or syngas). The reaction occurs on the catalysts typically composed of Ru,[5] Co,[6] Fe,[7] or Ni,[8]. The cobalt-based catalysts are commonly used as an industrial FTS catalyst because of its high selectivity to long chain hydrocarbons, a long catalyst life, and a reasonable material cost.[9] Metallic cobalt has been regarded as the active phase of cobalt-based catalysts in FTS reaction, so the reduction of cobalt without sintering is important to enhance the activity of cobalt-based FTS catalysts.[10] Because of the strong interaction with common oxide supports like SiO_2, Al_2O_3, and TiO_2, the cobalt species forms a spinel structure or other stable oxides, which are hardly reducible by the reduction pretreatment even at high temperatures (Scheme 1).[11] Typically promotion by noble metals such as Pt, Ru, and Re can lower the reduction temperature of cobalt species, which greatly elevates the catalytic activity of cobalt-based catalysts.[12] In the case of 100,000 bpd GTL process, 2.5 tons of platinum is required for catalyst per batch.[13] However, high price and scarcity of the noble metal[14] raise the operation cost of the whole process, which consequentially lower cost competitiveness of FTS products. Xiong *et al*.[15] reported the cobalt-based catalysts on the nitrogen-doped carbon spheres, which facilitate the reduction of cobalt resulting in improved FTS activity.

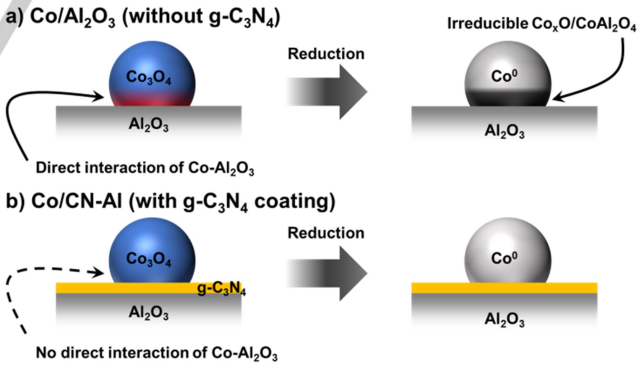

Scheme 1. Effect of the CN-Al support on the reducibility of cobalt species.

The graphitic carbon nitride (g-C_3N_4) is composed of carbon and nitrogen bonds with a graphene-like 2-dimensional (2-D) plane structure. It contains abundant nitrogen sites with lone pair electrons, which would function as basic sites for various reactions.[16] Also g-C_3N_4 has many defects at the edge of its plane. It is widely applied for various chemical and electro-catalytic reactions.[17] The synthesis of g-C_3N_4 is relatively simple, but its specific surface area is small because of the stacking and aggregation of the 2-D planes.[18] To increase the specific

[a] K. Y. Kim,[†] Dr. D. H. Youn, Prof. Dr. J. S. Lee
School of Energy and Chemical Engineering
Ulsan National Institute of Science and Technology (UNIST)
Ulsan, 689-798 (Korea)
E-mail: jlee1234@unist.ac.kr
[b] H. Park,[†] Dr. W. Y. Kim
Department of Chemical Engineering
Pohang University of Science and Technology (POSTECH)
Pohang, 790-784 (Korea)
[c] Y. H. Choi
Division of Advanced Nuclear Engineering
Pohang University of Science and Technology (POSTECH)
Pohang, 790-784 (Korea)
[†] These authors are contributed equally to this work.

Supporting information for this article is given via a link at the end of the document.

surface area of g-C_3N_4, the colloidal silica particles can be used as a nano-sized pore template, which is removed later by HF or NaOH treatment.[19]

Previously, we reported iron-based FTS catalysts over g-C_3N_4, in which g-C_3N_4 promoted the reduction of iron oxide and facilitated the formation Hägg iron carbide (χ-Fe_5C_2,), the active catalytic phase of the FTS reaction.[20] However, the structure of g-C_3N_4 was completely destroyed during the pretreatment and FTS reaction, and the iron particles were severely aggregated leading to the catalyst deactivation. In this work, we prepare g-C_3N_4 coated alumina support (CN-Al) for cobalt-based FTS catalyst, where g-C_3N_4 layers block the direct interaction between cobalt and alumina and facilitate the reduction of cobalt species (Scheme 1). Moreover, by using alumina as the stable support material, the catalyst maintains the high specific surface area and the small cobalt particle size during the reaction.

Results and Discussion

Catalyst preparation and characterization

The g-C_3N_4 was directly synthesized on alumina by using cyanamide precursor, which can be confirmed by XRD patterns in Figure S1. The prepared g-C_3N_4 coated alumina composite is denoted as xCN-Al (x = 6, 12, and 17), where x is weight % of g-C_3N_4 in CN-Al as determined by elemental analysis in Table 1. Surface morphology and crystalline structure of cobalt-loaded CN-Al (Co/CN-Al) catalysts and reference Co/Al_2O_3 was investigated by SEM and HRTEM analysis in Figure 1. The rough surface of CN-Al (Figure 1d) is attributed to the g-C_3N_4 debris on alumina while alumina itself has a smooth surface morphology (Figure 1a). The specific surface area of CN-Al composites decreases considerably with increasing amounts of g-C_3N_4 on Al_2O_3, and pores are also blocked by g-C_3N_4 coating (Figure S2 and Table S1). Therefore, the surface of Al_2O_3 is well covered by g-C_3N_4 coating in CN-Al, which would modify the physicochemical properties of alumina. When 20 wt. % of cobalt is loaded on the alumina support by impregnation, cobalt particles are severely aggregated giving 70-100 nm sizes (Figure 1b). The dispersion of cobalt is much improved on 17CN-Al with particle size decreasing to 15-20 nm (Figure 1e). The higher dispersion of cobalt species with addition of g-C_3N_4 on alumina could be attributable to a strong interaction between cobalt species and g-C_3N_4 on alumina surface, which retards the agglomeration of cobalt particles. After annealing under N_2 flow at 450 °C, the lattice distance of cobalt particle in Co/Al_2O_3 is 0.247 nm, which corresponds to the (113) facet of Co_3O_4 (Figure 1c). In contrast, the observed lattice distance in Co/CN-Al treated under the same conditions is 0.206 nm, which corresponds to (111) facet of metallic cobalt (Figure 1f). This unexpected result suggests that the cobalt species on CN-Al support can be reduced without hydrogen treatment.

The crystal structure of cobalt species in Co/Al_2O_3 was investigated by XRD in Figure 2. The species is Co_3O_4 as generally observed in calcined cobalt-based catalysts. The Co/6CN-Al catalyst also shows Co_3O_4 as the major phase, but

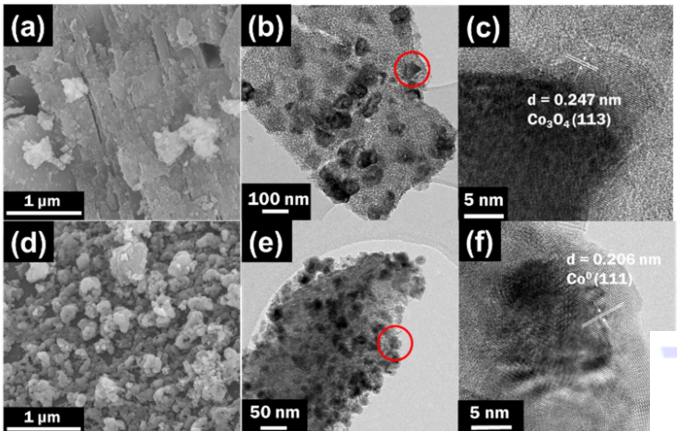

Figure 1. SEM images of bare Al_2O_3 (a) and 17CN-Al (d). HRTEM images of Co/Al_2O_3 (b, c) and Co/17CN-Al (e, f). The marked regions in (b) and (e) are magnified in (c) and (f), respectively.

Table 1. Properties of synthesized catalysts.

	surface area /m^2g^{-1}	N content / wt.%[a]	C+N content /wt.%[a]	Coba size/n
Co/Al_2O_3	117.61	-	-	8.85
Co/6CN-Al	128.81	4.26	6.34	5.03
Co/12CN-Al	116.09	7.97	12.02	7.00
Co/17CN-Al	123.26	11.07	17.04	13.40

[a]For bare CN-Al supports. [b]Measured by XRD. [c]Crystallite size of Co^0 calc from the obtained value of Co_3O_4 by Co^0 = 3/4 * Co_3O_4.[21] [d]Crystallite size of [e]Crystallite size of Co^0.

CoO with Co^0 peaks are observed as impurity phases. The Co/12CN-Al catalyst contains partially reduced cobalt (CoO) as the major phase. Finally, fully reduced cobalt becomes the major phase in Co/17CN-Al catalyst in agreement with the lattice distance exhibited in HRTEM images. The XRD patterns indicates that cobalt species in catalysts is in a more reduced form as the amount of g-C_3N_4 in the support increases, which is well represented in Figure 2b by decreasing peak intensity ratio of Co_3O_4/CoO and increasing Co^0/CoO with increasing g-C_3N_4 content in CN-Al composites. The annealing condition in our experiments (450 °C, 3 h, N_2 flow) is not supposed to form a reduced cobalt species. Yet it is remarkable that the extent of reduction of cobalt species can be controlled by the g-C_3N_4 content in the CN-Al support. The calculated crystallite size of cobalt by Scherrer's equation[22] increases from 8.85 nm for Co/Al_2O_3 to 13.4 nm for Co/17CN-Al (Table 1). The trend is not simple because of different oxidation states of cobalt species and specific surface areas (Table S1). Al_2O_3 has a larger surface area than CN-Al supports (Table S1), but Co/Al_2O_3 contains larger Co particles than those in Co/6CN-Al and Co/12CN-Al catalysts (Table 1). The result indicates that the strong interaction of Co and g-C_3N_4 is more important than the surface area of the support materials in the formation of small Co particles. More importantly, the secondary particle aggregation is

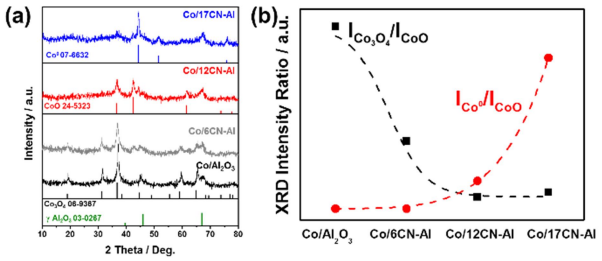

Figure 2. (a) XRD patterns for alumina-supported cobalt catalysts with different amounts of carbon nitride. (b) Comparisons of XRD peak intensity ratio of Co_3O_4/CoO (■) and Co^0/CoO (●). The peak intensity for Co_3O_4/CoO and Co^0/CoO ratios was obtained for peaks at 31°, 42°, and 44°, for Co_3O_4, CoO, and Co^0, respectively.

effectively retarded by coated g-C_3N_4 as revealed in HRTEM analysis in Figure 1.

In Figure 3a, the reduction behaviour of cobalt species in the catalysts is investigated by H_2-TPR analysis. The Co/Al_2O_3 catalyst gives two dominant peaks; at ~300 °C attributed to the reduction of Co_3O_4 to Co^0 and at 600 °C to the reduction of strongly bound Co_xO species on Al_2O_3 surfaces.[23] The intensity of the latter peak is dominant for Co/Al_2O_3 and Co/6CN-Al, but rapidly decreases with increasing amounts of g-C_3N_4 in the CN-Al supports. Typical reduction treatment in FTS process is below 400 °C, therefore a substantial fraction of the cobalt species is not reduced to metallic cobalt in Co-based FTS catalysts. Since metallic cobalt is the active phase for cobalt-based FTS catalysts, those unreduced cobalt oxide species such as Co_3O_4 and CoO cannot contribute to the FTS reaction.[10] Hence, the high content of cobalt species reduced below 400 °C is an important feature of the active Co-based FTS catalysts.

The fractions of peak areas below 400 °C of H_2-TPR spectra are presented in Figure 3b, which tend to increase with increasing g-C_3N_4 content in Co/CN-Al catalysts. In contrast, the total area of H_2-TPR peaks over whole temperature range (100–900 °C) decreases with g-C_3N_4 content. This indicates that some of cobalt species in Co/CN-Al catalysts has been already reduced during annealing procedure, which is in accordance with the XRD analysis. Thus, H_2-TPR indicates that g-C_3N_4 in the CN-Al support reduces the amount of irreducible cobalt species and facilitates the formation of metallic cobalt. Raman spectrum of Co/Al_2O_3 in Figure S3 exhibits Co-O stretching peaks of E_g, $F_{2g}^{(2)}$, $F_{2g}^{(3)}$, and A_{1g} at 472, 512, 610, and 682 cm^{-1}, respectively, for cobalt oxide species.[24] On the other hand, Co/CN-Al catalysts show slight red-shift by ~10 cm^{-1} of these Raman peaks. The red shift in Co-O stretching indicates weakened Co-O bonding in Co_xO species on CN-Al supports, thus its reduction to metallic cobalt becomes easier. Therefore, it is concluded that g-C_3N_4 on CN-Al support promotes the reduction of cobalt species as revealed by HRTEM, XRD, H_2-TPR, and Raman analyses.

Auto-reduction of cobalt on the graphitic carbon nitride

To investigate unusual reduction behaviour of cobalt under inert atmosphere on CN-Al supports, unannealed Co/CN-Al catalysts were analysed by the temperature-programmed reduction under helium flow (He-TPR) in Figure 4. There are complicated TCD

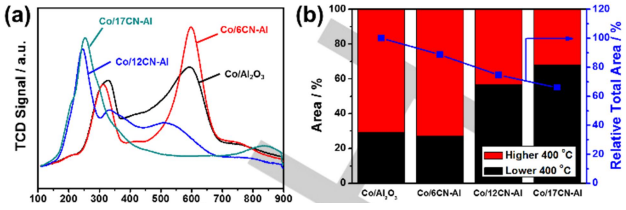

Figure 3. (a) H_2-TPR spectra and (b) fractions of peak area below 400 °C (black column) and relative total areas (■). Relative total area was calculated from total area of H_2-TPR in (a) and normalized with the area of Co/Al_2O_3 at 100 %.

signals below 300 °C, which are attributed to the decomposition of nitrate or various weakly adsorbed molecules on the CN-Al supports. The TCD signals in the range of 300-500 °C exhibit increasing peak intensity with increasing g-C_3N_4 contents and thus they should originate from the decomposition of g-C_3N_4 during He-TPR. This is convinced by elemental analyses of the samples upon interruption of He-TPR at different temperatures (Figure 5). The overall nitrogen and carbon content (C+N, wt.%) decreases as the He-TPR analysis progresses.

The two He-TPR peaks appearing at 350 and 460 °C suggests that two reactions occur at the temperatures. To investigate the processes occurring at 350 and 460 °C, He-TPR of Co/17CN-Al was interrupted at 280, 400, and 550 °C. The XRD pattern in Figure 4b of 280 °C sample exhibits Co_3O_4 as the only cobalt species. The Co/17CN-Al annealed by He-TPR up to 400 °C exhibits pure CoO. Finally in the 550 °C sample, the metallic cobalt species is observed. The XRD patterns of samples annealed at different temperatures indicate that the He-TPR peaks at 350 and 460 °C originate from the successive reduction of cobalt species, Co_3O_4 → CoO → metallic Co. Thus, the analyses clearly demonstrate that the decomposition of g-C_3N_4 accompany the reduction of cobalt species on the CN-Al support As shown in Figure 5, the content of nitrogen and carbon (N+C) continuously decreases with temperature increase during He-TPR, which is ascribed to the decomposition of g-C_3N_4. The nitrogen to carbon ratio (N/C), however, remains constant until 400 °C, then suddenly decreases after the second peak of He-TPR (550 °C). This implies that nitrogen is less stable than carbon under heat treatment leading to nitrogen deficient g-C_3N_4 at 450-500 °C (Scheme 2). Then, the neighbouring carbon atoms adjacent to nitrogen deficient site become unstable and easily reacts with oxygen atom in CoO resulting in completely reduced cobalt. This is supported by gas chromatography analysis, which indicates that the gaseous product evolving at 450 °C is CO (Figure S5). Yang *et al.*[25] reported the similar effect on the mesoporous carbon support, which was referred as 'auto-reduction behaviour'. The auto-reduction of cobalt oxide is caused by CO evolved from the decomposition of carbon supports. Thus mass spectroscopic CO evolution pattern reported by Cheng et al.[26] is similar to our He-TPR pattern of Co/CN-Al catalysts. The auto-reduction of cobalt on CN-Al supports (at 450 °C in Figure 4a) is much lower than that on nitrogen-doped carbon (500 °C). The enhanced reducibility is attributed to the reactive and unstable nature of nitrogen atoms in g-C_3N_4, which is easily decomposed to gaseous molecules. In auto-reduction of cobalt species on the carbon supports,

nitrogen doping is reported to be important to enhance the auto-reducibility of cobalt during the calcination in inert atmosphere.[15, 25a] The chemical structure of g-C_3N_4 is analogous to abundantly nitrogen-doped carbon materials, thus dominant nitrogen doping effect can be expected on the auto-reducibility.

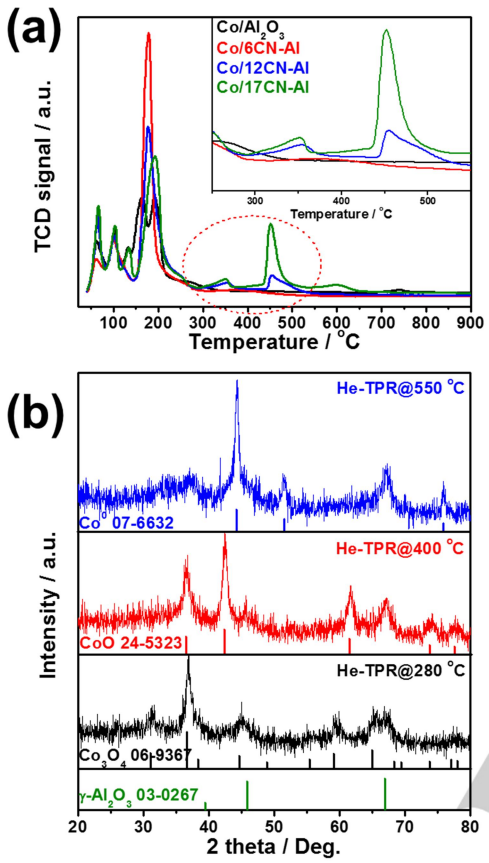

Figure 4. (a) He-TPR analysis for unannealed samples (b) XRD patterns of Co/17CN-Al catalysts during the interupted He-TPR.

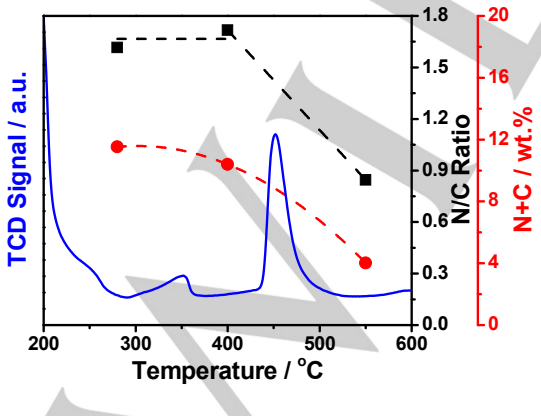

Figure 5. He-TPR (left scale) of Co/17CN-Al. N/C ratio (■) and total content of N and C (N+C/wt. %, ●) of Co/17CN-Al during He-TPR interrupted at 280, 400, and 550 °C.

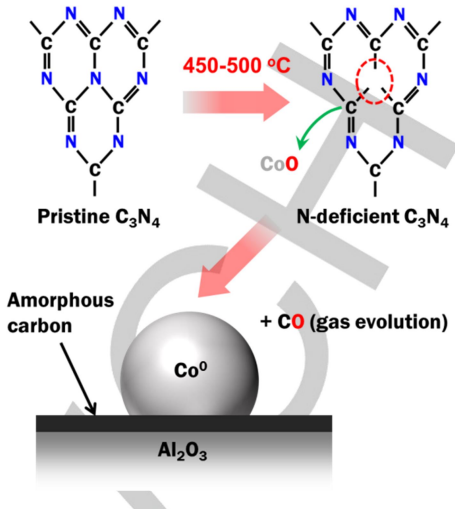

Scheme 2. The reduction mechanism of cobalt species under the inert gas flow for Co/CN-Al catalysts.

Degree of reduction of cobalt on graphitic carbon nitride

The degree of reduction (DOR) is quantified by O_2 pulse titration of the catalysts reduced at 400 °C by 10 vol. % H_2/Ar flow. It should be noted that g-C_3N_4 is fully combustible with O_2 below 400 °C (Figure S4), which is the experimental condition for O_2 pulse titration. The shoulder peaks at 200-350 °C in temperature programmed oxidation (TPO) in Figure S4 increase as the proportion of g-C_3N_4 in CN-Al support increases, indicating that g-C_3N_4 consumes oxygen below 400 °C. Therefore, the amount of O_2 consumption at the first titration must contain a portion for g-C_3N_4 combustion. Therefore, we denoted the first titration of Co/17CN-Al as '0th (zeroth)' to exclude the portion of g-C_3N_4 combustion, and the '1st and 2nd' are counted sequentially. The amount of consumed oxygen in the '1st' titration (25.4 μmol O_2) is quite lower than that of the '0th' titration (29.5 μmol O_2) because of the g-C_3N_4 combustion as mentioned above, but such difference disappears after the '2nd' titration (25.2 μmol O_2) Based on O_2 pulse titration results, DOR is calculated as 22.93 % for Co/17CN-Al, which is 1.54 times higher than that of Co/Al_2O_3 (14.88 %).

The improved DOR of cobalt species would increase the active sites in the catalysts for FTS reaction. Typical oxide support materials such as SiO_2, Al_2O_3, and TiO_2 have a strong interaction with cobalt species in the catalysts, which retards the reduction of cobalt during the hydrogen reduction step and the catalytic reaction. Therefore, even after the reduction treatment, there is irreducible cobalt species in the catalyst which is inactive for FTS reaction. On the surface of CN-Al support, however, g-C_3N_4 blocks the direct contact of Al_2O_3 and cobalt species to hinder the formation of irreducible cobalt species and, in addition, directly reduces the cobalt species along with its decomposition. Hence the reducibility of cobalt is much improved by using CN-Al support.

Table 2. Degree of reduction (DOR) of catalysts by O_2 pulse titration.

Catalysts	Consumed O_2 titration / μmol O_2			DOR[b] /%
	0th[a]	1st	2nd	
Co/Al_2O_3	-	14.9	16.5	14.88
Co/17CN-Al	29.5	25.4	25.2	22.93

Pretreatment: ramping rate of 5 °C min^{-1}, 400 °C, 3 h, 50 ml min^{-1} 10 vol. % H_2/Ar flow. Titration condition: 400 °C, 50 ml min^{-1} He flow, 5 vol. % O_2/He pulse injection. The pretreatment and titration are repeated until the 2nd titration is completed. [a]The O_2 consumption of the 0th titration contains contribution of the g-C_3N_4 combustion by O_2 (see the text). [b]DOR is calculated based on the average value of the 1st and 2nd O_2 titration for each catalyst.

Catalytic Fischer-Tropsch reaction

Catalytic FTS reaction was performed in a 1/2 inch stainless steel fixed bed reactor at 220 °C, 20 bar, and H_2/CO = 2 over Co/17CN-Al and Co/Al_2O_3 to demonstrate the effect of g-C_3N_4 coating on the alumina surface. The Co/17CN-Al catalyst demonstrates a stable activity of CO hydrogenation for 50 h of continuous operation as in Figure 6. The cobalt time yield (CTY) of Co/17CN-Al at 50 h of time on stream (TOS) is 21.84 μmol s^{-1} g_{Co}^{-1}, which is twice higher than that of Co/Al_2O_3 (10.75 μmol s^{-1} g_{Co}^{-1}). Notably, the catalytic activity of Co/g-C_3N_4 without Al_2O_3 is lower than Co/Al_2O_3 because of the severe aggregation of cobalt as g-C_3N_4 is destroyed during the pretreatment (Figure S7). The enhanced activity of Co/17CN-Al is mainly due to the improved reducibility of cobalt species as discussed above. Since the metallic cobalt is the active phase for the cobalt-based FTS catalyst, the catalysts should be treated under reductive condition to generate the metallic cobalt prior to the FTS reaction. However, cobalt species in Co/17CN-Al is already reduced during the annealing process, and thus it does not need to be reduced before the FTS reaction. Thus, the Co/17CN-Al catalyst pretreated under Ar flow exhibited almost the same CTY as that of H_2 treated Co/CN-Al. In contrast, when the Co/Al_2O_3 is treated with Ar, the activity drops drastically due to the unreduced cobalt species in the catalyst. Therefore, the enhanced reducibility and carbothermal reduction induced by g-C_3N_4 result in improved catalytic activity on the FTS reaction for Co/17CN-Al catalysts and the catalyst does not need reduction treatment prior to the FTS reaction which would lower the operating cost for FTS process. The XRD pattern of used Co/Al_2O_3 show the metallic cobalt species generated during the reaction (Figure S6). However the catalytic activity is still lower than Co/17CN-Al, which suggests that the improved dispersion of cobalt species on CN-Al support is also the reason for the enhanced activity.

Conclusions

The effects of g-C_3N_4 coating on the typical alumina support have been investigated for cobalt-based FTS catalysts. The g-C_3N_4 was successfully synthesized *in situ* on the alumina surface, which was verified by XRD, BET, and SEM analysis. The g-C_3N_4 coating on the alumina surface retards the aggregation of cobalt particles and improves the cobalt dispersion. Direct contact of cobalt and alumina is blocked by g-C_3N_4 coating on CN-Al support, which reduces formation of irreducible cobalt oxide species. Moreover, g-C_3N_4 is decomposed under inert condition during the initial annealing step to produce carbon monoxide that directly reduces the cobalt species to metallic cobalt even without hydrogen treatment. This auto-reduction of cobalt oxide species is facilitated by unstabilized carbon species adjacent to defective nitrogen sites in g-C_3N_4. As much more reduced cobalt sites are formed on CN-Al support, FTS activity of Co/CN-Al catalysts is improved and remains stable for 50 h of continuous operation. Because of the readily formed metallic cobalt on CN-Al support under inert condition, the high FTS activity is obtained without pre-reduction by hydrogen. The reduction promotion by expensive noble metals like Pt is not needed either. By using the CN-Al support, pretreatment process for cobalt activation

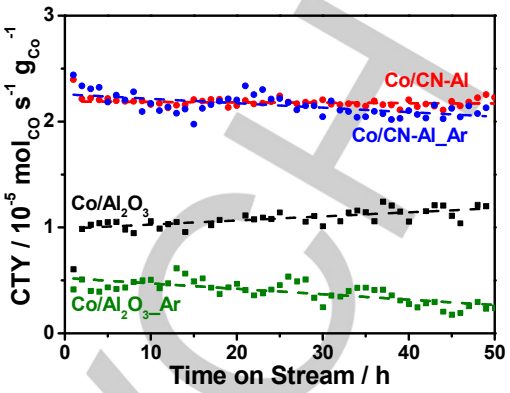

Figure 6. Cobalt time yield (CTY, mol_{CO} s^{-1} g_{co}^{-1}) for the FTS reaction with time on stream. Reaction conditions: 220 °C, 20 bar, H_2/CO=2.

Table 3. Catalytic performance in the FTS reaction.[a]

Catalysts	CTY / μmols^{-1} g_{Co}^{-1}	CO_2 sel./%	CO_2-free HC sel./%			O/P
			CH_4	C_2-C_4	C_{5+}	
Co/Al_2O_3_H_2	10.75	2.358	10.90	8.46	80.64	1.539
Co/Al_2O_3_Ar	3.92	24.10	26.15	39.79	34.06	0.886
Co/17CN-Al_H_2	21.84	2.900	9.08	13.12	77.80	2.106
Co/17CN-Al_Ar	21.52	7.744	9.92	14.29	75.79	1.812

[a]The results were obtained at steady state at least 50 h of time on stream. [b]The O/P ratio was calculated for C_2-C_4 hydrocarbon products. Reaction conditions: 220 °C, 20 bar, H_2/CO = 2, CO conversion = 14±2 %.

becomes much simpler and cheaper, and the activity is also much enhanced.

Experimental Section

Preparation of carbon nitride coated alumina (CN-Al). Carbon nitride coated aluminium oxide support was prepared by direct synthesis of carbon nitride from cyanamide (CA, Aldrich) on γ-Al_2O_3 (Aldrich). CA was dissolved in deionized water and mixed with γ-Al_2O_3. With vigorous stirring, the mixture was heated to evaporate water. Then, the powder was heated to 550 °C (4.58 °C min^{-1}) for 4 h under N_2 flow (100 ml min^{-1}). Three kinds of the carbon nitride coated alumina were prepared with different CA/Al_2O_3 weight ratios, denoted as xCN-Al (x= 6, 12, and 17 for CA/Al_2O_3 of 0.8/1.6, 0.6/1.7, and 0.4/1.8, respectively. The value x was the weight percent of g-C_3N_4 in CN-Al.).

Impregnation of support materials with cobalt. 20 wt. % of cobalt was loaded by a typical incipient wetness impregnation method using cobalt nitrate hexahydrate (Aldrich) as a cobalt precursor. The catalysts were heated at 450 °C for 3 h under N_2 flow (100 ml min^{-1}).

General characterization. HRTEM images were obtained using the instrument in UNIST Central Research Facility (JEM2100F, JEOL). SEM images were obtained using a Quanta 200FEG, FEI instrument. X-ray diffraction patterns (XRD) were measured on PANalytical PW 3040/60 X'pert. The chemical composition of materials was measured by element analyzer (EA, Truspec Micro, Leco), and inductively couples plasma (ICP, 700-ES, Varian). The oxidation state of surface elements was measured by X-ray photoelectron spectroscopy (XPS, K-alpha, ThermoFisher). The specific BET surface area was measured by N_2 physisorption isotherm at -196 °C (Nanoporosity-XQ, Mirae SI). Raman spectra were measured at room temperature with 532 nm radiation laser, Nd-doped yttrium aluminium garnet, 1 mW potency, CCD type detector, 800 nm spot diameter with 9 distinguished spots for each sample (alpha300R, WITec).

Temperature-programmed reductions and oxidation. Evolution of products during the H_2-temperature-programmed reduction (H_2-TPR), He-TPR, temperature-programmed oxidation (TPO), and O_2 pulse titration were monitored by a thermal conductivity detector (TCD, AutoChem 2920, Micrometrics). The samples were pretreated at 200 °C for 2 h under Ar flow (50 ml min^{-1}) and then cooled down to ambient temperature. The TCD signal was recorded with temperature ramp to 900 °C at 10 °C/min under 10 vol. % H_2/Ar (50 ml min^{-1}) flow. He-TPR was performed by using uncalcined samples with a ramping rate of 5 °C min^{-1} and He flow of 50 ml min^{-1}. TPO was measured under 5 vol. % O_2/He flow (50 ml min^{-1}). Degree of reduction of cobalt in catalysts was measured by O_2 pulse titration at 400 °C under 5 vol. % O_2/He flow (50 ml min^{-1}). It was assumed that all reduced cobalt species formed during the hydrogen treatment (400 °C, 3 h, 50 ml min^{-1}) were sufficiently oxidized by 150 pulses of O_2.

Catalytic performance test of FTS reaction

Catalytic performance was tested in 1/2 inch stainless steel fixed bed reactor under simulated industrial condition (20 bar, 220 °C and H_2/CO = 2). The catalyst was mixed with 3.0 g of SiC (Aldrich) as diluent to prevent the formation of hot spot in the catalytic bed. Catalysts were pre-treated under hydrogen flow (50 ml min^{-1}) at ambient pressure and 400 °C (5 °C min^{-1}) for 3 h, then the reactor was cooled down to 200 °C (2.22 °C min^{-1}) and argon was filled until the pressure reaches 20 bar. After waiting 1 h for stabilization of the temperature, reactant gases (H_2/CO/N_2 = 63.8/31.9/4.3 vol. %) were introduced and the catalysts were aged for 12 h. Finally, the temperature was slowly increased to 220 °C (0.5 °C min^{-1}), and CO conversion was controlled by adjusting the gas flow rate. The catalytic performance was measured at a fixed CO conversion of 14±2 % in order to exclude the effect of conversion on selectivity. The CO conversion was controlled by adjusting the gas flow rate. The liquid and wax products were collected by hot trap (150 °C, 20 bar) and cold trap (1 °C, 1 bar), respectively. The gaseous products were analysed by on-line connected gas chromatography (GC, 7890A, Agilent technologies) equipped with 60/80 Carboxen 1000 column.

Acknowledgements

This research was supported by the Climate Change Response project (2015M1A2A2074663, 2015M1A2A2056824), the Basic Science Grant (NRF-2015R1A2A1A10054346), Korea Center for Artificial Photosynthesis (KCAP, No. 2009-0093880) funded by MSIP, Project No. 10050509 and KIAT N0001754 funded by MOTIE of Republic of Korea.

Keywords: Fischer-Tropsch synthesis • auto-reduction • cobalt • carbon nitride • reducibility

[1] K. S. Deffeyes, *Hubbert's Peak: The Impending World Oil Shortage*, 1st ed., Prinston University Press, New Jersey, **2001**.
[2] M. S. Dresselhaus, I. L. Thomas, *Nature* **2001**, *414*, 332-337.
[3] a) A. d. K. Peter M. Maitlis, *Greener Fischer-Tropsch Processes for Fuels and Feedstocks*, Wiley-VCH Verlag GmbH & Co. KGaA, Weinheim, **2013**; b) S. Shafiee, E. Topal, *Energy Policy* **2009**, *37*, 181-189.
[4] a) B. I. Kamara, J. Coetzee, *Energy Fuels* **2009**, *23*, 2242-2247; b) O. Armas, K. Yehliu, A. L. Boehman, *Fuel* **2010**, *89*, 438-456.
[5] C. Xiao, Z. Cai, T. Wang, Y. Kou, N. Yan, *Angew. Chem. Int. Ed.* **2008**, *47*, 746-749.
[6] E. Iglesia, *Appl. Catal. A: Gen.* **1997**, *161*, 59-78.
[7] H. M. Torres Galvis, J. H. Bitter, C. B. Khare, M. Ruitenbeek, A. I. Dugulan, K. P. de Jong, *Science* **2012**, *335*, 835.
[8] L. Bruce, J. F. Mathews, *Appl. Catal.* **1982**, *4*, 353-369.
[9] A. Y. Khodakov, W. Chu, P. Fongarland, *Chem. Rev.* **2007**, *107*, 1692-1744.
[10] A. Y. Khodakov, *Catal. Today* **2009**, *144*, 251-257.
[11] G. Jacobs, T. K. Das, Y. Zhang, J. Li, G. Racoillet, B. H. Davis, *Appl. Catal. A: Gen.* **2002**, *233*, 263-281.
[12] a) S. Vada, A. Hoff, E. Ådnane, S. D. Schanke, A. Holmen, *Top. Catal.* **1995**, *2*, 155-162; b) W. Chu, P. A. Chernavskii, L. Gengembre, G. A. Pankina, P. Fongarland, A. Y. Khodakov, *J. Catal.* **2007**, *252*, 215-230; c) A. Kogelbauer, J. J. G. Goodwin, R. Oukaci, *J. Catal.* **1996**, *160*, 125-133.
[13] A. Brumby, M. Verhelst, D. Cheret, *Catal. Today* **2005**, *106*, 166-169.
[14] P. C. K. Vesborg, T. F. Jaramillo, *RSC Adv.* **2012**, *2*, 7933-7947.
[15] H. Xiong, M. Moyo, M. K. Rayner, L. L. Jewell, D. G. Billing, N. J. Coville, *ChemCatChem* **2010**, *2*, 514-518.
[16] X. Jin, V. V. Balasubramanian, S. T. Selvan, D. P. Sawant, M. A. Chari, G. Q. Lu, A. Vinu, *Angew.Chem. Int. Ed.* **2009**, *48*, 7884-7887.
[17] Y. Zheng, J. Liu, J. Liang, M. Jaroniec, S. Z. Qiao, *Energy Env.Sci.* **2012**, *5*, 6717-6731.
[18] P. Niu, L. Zhang, G. Liu, H.-M. Cheng, *Adv. Funct.Mater.* **2012**, *22*, 4763-4770.
[19] a) A. Vinu, K. Ariga, T. Mori, T. Nakanishi, S. Hishita, D. Golberg, Y. Bando, *Adv. Mater.* **2005**, *17*, 1648-1652; b) F. Goettmann, A. Fischer, M. Antonietti, A. Thomas, *Angew. Chem. Int.Ed.* **2006**, *45*, 4467-4471.
[20] H. Park, D. H. Youn, J. Y. Kim, W. Y. Kim, Y. H. Choi, Y. H. Lee, S. H. Choi, J. S. Lee, *ChemCatChem* **2015**, *7*, 3488-3494.
[21] D. Schanke, *J. Catal.***1995**, *156*, 85-95.

[22] A. L. Patterson, *Phys. Rev.* **1939**, *56*, 978-982.
[23] S. M. Olusola O. James, *J. Pet. Technol. Altern. Fuels* **2016**, *7*, 1-12.
[24] B. Jongsomjit, C. Sakdamnuson, J. G. Goodwin, P. Praserthdam, *Catal. Lett.* **2004**, *94*, 209-215.
[25] a) Y. Yang, L. Jia, B. Hou, D. Li, J. Wang, Y. Sun, *ChemCatChem* **2014**, *6*, 319-327; b) Y. Yang, L. Jia, B. Hou, D. Li, J. Wang, Y. Sun, *Catal. Sci. Tech.* **2014**, *4*, 717-728.
[26] K. Cheng, V. Subramanian, A. Carvalho, V. V. Ordomsky, Y. Wang, A. Y. Khodakov, *J. Catal.* **2016**, *337*, 260-271.

Entry for the Table of Contents (Please choose one layout)

Layout 1:

FULL PAPER

Text for Table of Contents

g-C_3N_4 coated on Al_2O_3 blocks the interaction between Co and Al_2O_3 and is decomposed to evolve reductive CO gas to generate the metallic cobalt even under the inert conditions. The improved reducibility of the cobalt species on g-C_3N_4/Al_2O_3 raises the the catalytic activity of Co in the Fischer-Tropsch synthesis.

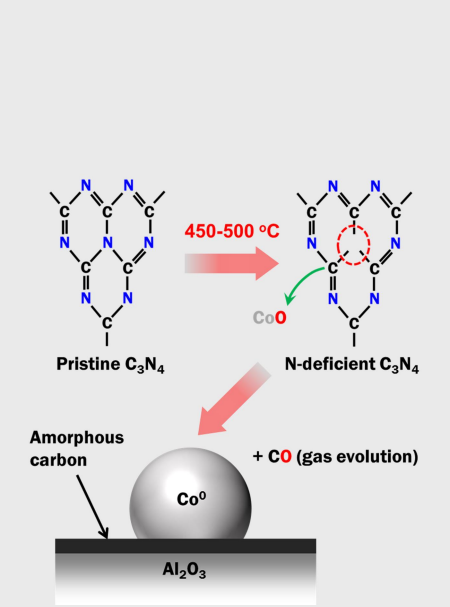

*Hunmin Park, Kwang Young Kim, Duck Hyun Youn, Yo Han Choi, Won Young Kim, and Jae Sung Lee**

Page No. – Page No.

Title
Auto-reduction Behaviour of Cobalt on Graphitic Carbon Nitride Coated Alumina Supports for Fischer-Tropsch Synthesis